Molecules and Cells

Rev-erbα Negatively Regulates Osteoclast and Osteoblast Differentiation through p38 MAPK Signaling Pathway

Kabsun Kim[1], Jung Ha Kim[1], Inyoung Kim[1], Semun Seong[1,2], and Nacksung Kim[1,2,*]

[1]Department of Pharmacology, Chonnam National University Medical School, Gwangju 61469, Korea, [2]Department of Biomedical Sciences, Chonnam National University Medical School, Gwangju 61469, Korea
*Correspondence: nacksung@jnu.ac.kr
https://doi.org/10.14348/molcells.2019.0232
www.molcells.org

The circadian clock regulates various physiological processes, including bone metabolism. The nuclear receptors Rev-erbs, comprising Rev-erbα and Rev-erbβ, play a key role as transcriptional regulators of the circadian clock. In this study, we demonstrate that Rev-erbs negatively regulate differentiation of osteoclasts and osteoblasts. The knockdown of Rev-erbα in osteoclast precursor cells enhanced receptor activator of nuclear factor-κB ligand (RANKL)-induced osteoclast formation, as well as expression of nuclear factor of activated T cells 1 (NFATc1), osteoclast-associated receptor (OSCAR), and tartrate-resistant acid phosphatase (TRAP). The overexpression of Rev-erbα leads to attenuation of the NFATc1 expression via inhibition of recruitment of c-Fos to the NFATc1 promoter. The overexpression of Rev-erbα in osteoblast precursors attenuated the expression of osteoblast marker genes including Runx2, alkaline phosphatase (ALP), bone sialoprotein (BSP), and osteocalcin (OC). Rev-erbα interfered with the recruitment of Runx2 to the promoter region of the target genes. Conversely, knockdown of Rev-erbα in the osteoblast precursors enhanced the osteoblast differentiation and function. In addition, Rev-erbα negatively regulated osteoclast and osteoblast differentiation by suppressing the p38 MAPK pathway. Furthermore, intraperitoneal administration of GSK4112, a Rev-erb agonist, protects RANKL-induced bone loss via inhibition of osteoclast differentiation *in vivo*. Taken together, our results demonstrate a molecular mechanism of Rev-erbs in the bone remodeling, and provide a molecular basis for a potential therapeutic target for treatment of bone disease characterized by excessive bone resorption.

Keywords: bone remodeling, osteoblast, osteoclast, p38 MAPK, Rev-erb

INTRODUCTION

Mammalian circadian clock genes regulate the circadian rhythms characterized by periodic physiological and behavioral changes that help an organism achieve the optimization of metabolism and energy utilization (Reppert and Weaver, 2002; Schibler and Sassone-Corsi, 2002). The clock genes, located centrally in the suprachiasmatic nucleus (SCN) of the brain, are also involved in the control of homeostasis in peripheral tissues and organs, and play a tissue-specific role, independently from the SCN, in various physiological processes, including bone formation (McDearmon et al., 2006; Wu et al., 2008). It has been reported that circadian clocks maintain bone remodeling by regulating bone formation and resorption (Xu et al., 2016).

The circadian clock mechanism includes an interconnected transcriptional and translational feedback loop, in which

Received 14 October, 2019; revised 21 November, 2019; accepted 1 December, 2019; published online 3 January, 2020

eISSN: 0219-1032

the most well-known positive regulator is a heterodimer of BMAL1 and CLOCK. In addition to positively regulating the clock output genes, the BMAL1/CLOCK heterodimer activates the expression of two negative regulators, PERIOD (PER) and CRYPTOCHROME (CRY) (Kim et al., 2018; King and Takahashi, 2000). In a negative feedback loop, PER and CRY interact with the BMAL1/CLOCK heterodimer and interfere with its transcriptional activity. An additional essential negative feedback loop is mediated by transcriptional repression of the nuclear receptors Rev-erbs (Lazar et al., 1989; Liu et al., 2008).

The nuclear receptors Rev-erbα and Rev-erbβ regulate several physiological processes including circadian rhythm, metabolism, and inflammatory responses (Ramakrishnan and Muscat, 2006). Rev-erbs lack the carboxy-terminal tail of the ligand-binding domain that is required for ligand-dependent transcriptional activation by other nuclear receptors. Thus, Rev-erbs were considered as constitutive repressors of transcription based on their ability to recruit corepressors and suppress the transcription of the target genes (Harding and Lazar, 1993; Zamir et al., 1997). Due to the limited availability of genetic models in exploring the function of Rev-erbβ, the role of Rev-erbα in mammalian circadian and metabolic physiologies is comparatively well-known. Accordingly, Rev-erbβ is considered functionally redundant to Rev-erbα and its role has been considered almost identical to that of Rev-erbα (Duez and Staels, 2009).

The bones are maintained by continuous remodeling throughout life, which includes the removal of mature bone by osteoclasts followed by the formation of new bone by osteoblasts. The processes of bone resorption and bone formation balance each other in order to maintain constant bone mass. An imbalance between the two processes results in bone metabolic disorders such as osteoporosis.

Osteoclasts are multinucleated giant cells derived from hematopoietic progenitor cells in the presence of macrophage colony stimulating factor (M-CSF) and the receptor activator of nuclear factor-κB ligand (RANKL). RANKL binds to its receptor, receptor activator of NF-κB (RANK), and promotes osteoclast formation via activation of various signaling molecules such as NF-κB, activator protein-1 (AP-1), and mitogen-activated protein kinases (MAPKs) including p38, extracellular signal-regulated kinase (ERK), and c-Jun N-terminal kinase (JNK). The signal transduction process induces expression of osteoclast marker genes such as nuclear factor of activated T cells 1 (NFATc1), osteoclast-associated receptor (OSCAR), and tartrate-resistant acid phosphatase (TRAP) (Kim and Kim, 2016; Roodman, 2006).

Osteoblasts are derived from mesenchymal stem cells (MSCs) and their differentiation is regulated by a number of hormones and factors, such as bone morphogenetic proteins (BMPs), wingless and int-1 (Wnt), and insulin-like growth factor (IGF) (Cao and Chen, 2005; Day et al., 2005). The runt-related transcription factor 2 (Runx2) is a major transcription factor in osteoblast differentiation that up-regulates the transcription of genes required for bone matrix deposition and mineralization including alkaline phosphatase (ALP), osteocalcin (OC), and bone sialoprotein (BSP), which are key regulators of osteoblast differentiation and function (Komori, 2011). The osteogenic factors activate ERK, JNK, and p38 kinase signaling pathways, which are involved in the induction and control of Runx2 transcriptional activity (Lee et al., 2018; Rodriguez-Carballo et al., 2016; Sowa et al., 2002; Xiao et al., 2002; Ziros et al., 2002). The function of Rev-erbα in osteoclast and osteoblast has been reported previously, while little is known about the molecular mechanism of Rev-erbs in bone metabolism (He et al., 2015; Song et al., 2018).

In this study, we investigated the role of Rev-erbs on osteoclastogenesis and osteoblastogenesis *in vitro* and *in vivo* and elucidated its underlying molecular mechanisms. The gain of function and loss of function analysis of Rev-erbs suggested that Rev-erbα acts as a negative regulator in both osteoclasts and osteoblasts accompanied by inhibition of p38 MAPK signaling cascade. We observed the functional redundancy of Rev-erbβ to Rev-erbα in osteoclast differentiation, but not in osteoblast differentiation. Further understanding of the molecular mechanisms of Rev-erbα in bone metabolism will provide useful information regarding potential therapeutic targets for treatment of bone diseases.

MATERIALS AND METHODS

Reagents

Cell culture media and supplements were obtained from HyClone Laboratories (USA). Recombinant human M-CSF and RANKL were purified from bacteria. IGF-1, GSK4112, alizarin red, β-glycerophosphate, and p-nitrophenyl phosphate were obtained from Sigma-Aldrich (USA). Recombinant human BMP2 was purchased from Cowellmedi (Korea). Ascorbic acid was purchased from Junsei Chemical (Japan).

Animals

All mice handling and experiments were performed as per guidelines of the National Institutes of Health (Guide for the Care and Use of Laboratory Animals). The experimental protocol was approved by the Chonnam National University Medical School Research Institutional Animal Care and Use Committee (CNU IACUC-H-2017-27).

Osteoclast differentiation and TRAP staining

Murine osteoclasts were prepared from bone marrow cells, which were obtained by flushing the femurs and tibiae from 6-week-old male Institute of Cancer Research (ICR) mice. The bone marrow cells were cultured in α-MEM containing 10% fetal bovine serum (FBS) with M-CSF (30 ng/ml) for 3 days, and the bone marrow-derived macrophage-like cells (BMMs) were used as the osteoclast precursors. To generate osteoclasts, the BMMs were cultured with M-CSF (30 ng/ml) and RANKL (100 ng/ml) for 3 days at 37°C and 5% CO_2. The cultured cells were fixed and stained for TRAP. TRAP-positive multinuclear cells that contained more than three nuclei were denoted as osteoclasts. The cells were observed using the Leica DM IRB microscope equipped with an N plan 10 × 0.25 numerical aperture objective lens (Leica Microsystems, Germany). The images were obtained using the ProgRes CFscan camera, and the ProgRes CapturePro software (Jenoptik, Germany).

Osteoblast differentiation

Mouse bone marrow stromal cells were isolated by flushing the femurs and tibiae from 6-week-old male ICR mice, and the isolated cells were cultured in α-MEM containing 10% FBS, 100 U/ml penicillin, and 100 μg/ml streptomycin. Osteoblast differentiation was induced by incubating the cells in an osteogenic medium containing 50 ng/ml IGF-1, 50 μg/ml ascorbic acid, and 100 μM β-glycerophosphate for 4 to 9 days; the culture medium was replaced every 4 days for the ALP activity assay. The osteoblast precursor cells were lysed using the osteoblast lysis buffer (50 mM NaCl [pH 7.6], 150 mM NaCl, 0.1% Triton X-100, and 1 mM EDTA). The cell lysates were incubated with p-nitrophenyl phosphate substrate (Sigma-Aldrich), and ALP activity was measured using a spectrophotometer at 405 nm. For alizarin red staining, the cells were cultured for 9 days, and were fixed with 70% ethanol and stained with 40 mM alizarin red (pH 4.2). The nonspecific staining was removed by phosphate-buffered saline (PBS) wash, and alizarin red staining was visualized with a CanoScan 4400F scanner (Canon, Japan). Alizarin red was then dissolved using 10% Cetylpyridinium (Sigma-Aldrich) for 15 min at room temperature, and alizarin red activity was measured using a spectrophotometer at 562 nm.

Cytotoxicity assay

The bone marrow cells were seeded in 96-wells plates with α-MEM containing 10% FBS with M-CSF. The cells were treated with different concentrations of GSK4112 for 2 days in presence of M-CSF and RANKL. Next, the cells were incubated with 10% EZ-Cytox reagent (DaeilLab Service, Korea) for 4 h at 37°C and 5% CO_2, the number of viable cells in triplicate wells was measured with a spectrophotometer at 450 nm.

Semi quantitative real-time polymerase chain reaction (PCR)

Cells were lysed in Qiazol (Qiagen, Germany), and total RNA was isolated according to the manufacturer's protocol. Purified RNA was reverse transcribed with GoScript™ Reverse Transcriptase (Promega, USA), and the resultant cDNA was used for SYBR-based real-time PCR. The assays were performed in triplicates with a Rotor-Gene6 instrument (Qiagen). The thermal cycling conditions were as follows: 15 min at 95°C, followed by 40 cycles of 94°C for 15 s, 55°C for 30 s, and 72°C for 30 s. Total mRNA was normalized to the endogenous housekeeping gene *Gapdh*. The relative quantitation value for each target gene was expressed as $2^{(Ct\ Cc)}$ (Ct and Cc are the mean threshold cycle differences after normalizing to *Gapdh*). The relative expression levels of samples were represented by a semi-log plot. The following primer sets were used: Rev-erbα: forward, 5′-GAC CCT GGA CTC CAA TAA CAA CA-3′; reverse, 5′-GGT AAT GTT GCT TGT GCC CTT GC-3′; Rev-erbβ: forward, 5′-GTG TGA TTG CCT ACA TCA GTT CC-3′; reverse, 5′-CAG GCA CTT CTT ATA CTG GAT GT-3′; c-fos: forward, 5′-ATG GGC TCT CCT GTC AAC ACA CAG-3′; reverse, 5′-TGG CAA TCT CAG TCT GCA ACG CAG-3′; Nfatc1: forward, 5′-CTC GAA AGA CAG CAC TGG AGC AT-3′; reverse, 5′-CGG CTG CCT TCC GTC TCA TAG-3′; Oscar: forward, 5′-TGC TGG TAA CGG ATC AGC TCC CCA A-3′; reverse, 5′-CCA AGG AGC CAG AAC CTT CGA AAC T-3′; Acp5: forward, 5′-CTG GAG TGC ACG ATG CCA GCG ACA-3′; reverse, 5′-TCC GTG CTC GGC GAT GGA CCA GA-3′; Ctsk: forward, 5′-ACG GAG GCA TTG ACT CTG AAG ATG-3′; reverse, 5′-GTT GTT CTT ATT CCG AGC CAA GAG-3′; Dc-stamp: forward, 5′-TGG AAG TTC ACT TGA AAC TAC GTG-3′; reverse, 5′-CTC GGT TTC CCG TCA GCC TCT CTC-3′; Alpl: forward, 5′-CAA GGA TAT CGA CGT GAT CAT G-3′; reverse, 5′-GTC AGT CAG GTT GTT CCG ATT C-3′; Runx2: forward, 5′-CCC AGC CAC CTT TAC CTA CA-3′; reverse, 5′-CAG CGT CAA CAC CAT CAT TC-3′; Ibsp: forward, 5′-GGA AGA GGA GAC TTC AAA CGA A-3′; reverse, 5′-CAT CCA CTT CTG CTT CTT CGT TC-3′; Bglap: forward, 5′-ATG AGG ACC CTC TCT CTG CTC AC-3′; reverse, 5′-CCA TAC TGG TTT GAT AGC TCG TC-3′; Gapdh: forward, 5′-TGA CCA CAG TCC ATG CCA TCA CTG-3′; reverse, 5′-CAG GAG ACA ACC TGG TCC TCA GTG-3′.

Retroviral infection

The Plat-E packaging cells were maintained in Dulbecco's modified Eagle's medium (DMEM) supplemented with 10% FBS. To prepare retroviral supernatants, recombinant plasmids and parental pMX vectors were transfected into the packaging cell line Plat-E using FuGENE 6 (Promega) according to the manufacturer's instructions. The viral supernatant was collected from the cultured media 48 h after transfection. The BMMs or osteoblast precursor cells were incubated with the viral supernatants for 6 h in the presence of 10 μg/ml polybrene (Sigma-Aldrich).

Luciferase assay

293T cells were cultured in DMEM supplemented with 10% FBS. The cells were transfected with the indicated amounts of expression plasmids using FuGENE 6 (Promega), according to the manufacturer's protocol. On the following day, the cells were treated with compounds and after 24 h luciferase activities were measured according to the manufacturer's instructions (Promega). The Luciferase activity was measured in triplicates, which were averaged and normalized to the β-galactosidase activity using o-nitrophenyl-β-D-galactopyranoside (Sigma-Aldrich) as a substrate.

Small interfering RNA transfection

Control siRNA, Rev-erbα siRNA, and Rev-erbβ siRNA purchased from Dharmacon (USA) were transfected into BMMs or preosteoblasts using Lipofectamine RNAiMAX (Thermo Fisher Scientific, USA), according to the manufacturer's protocol. The knockdown was verified by quantitative PCR.

Immunoprecipitation and western blot analysis

Cells from the transfected 293T, osteoclasts, or osteoblasts were harvested after washing with ice-cold PBS, and were lysed using extraction buffer (50 mM Tris-HCl [pH 8.0], 150 mM NaCl, 1 mM EDTA, 0.5% Nonidet P-40, 0.01% protease inhibitor cocktail). The samples were immunoprecipitated with antibodies, and the whole cell lysates were subjected to SDS-PAGE and western blotting. The primary antibodies used included Rev-erbα (E-12, #sc-393215, 1:1,000), Rev-erbβ (E-12, #sc-393215, 1:1,000), c-Fos (K-25, #sc-

253,1:1,000), NFATc1 (7A6, #sc-7294, 1:1,000), TRAP (H-274, sc-274, 1:1,000), Runx2 (M70, #sc-10758, 1:1,000), Tubulin (#sc-58884, 1:1,000), LaminB1 (#sc-56143,1:1,000) phospho-Smad (#12353, 1:1,000), and Smad (N-18, #sc-6031, 1:1,000) antibodies (Santa Cruz Biotechnology, USA). IκB (#9242, 1:1,000), phospho-p38 (#9211, 1:1,000), p38 (#9212, 1:1,000), phospho-JNK (G9, #9255, 1:1,000), JNK (#9252, 1:1,000), phospho-ERK (#9101, 1:1,000), and ERK (#9102, 1:1,000) antibodies (Cell Signaling Technology, USA). In addition, Actin (Clone AC-40, #A8353, 1:25,000) and Flag (Clone M2, #A8592, 1:3,000) antibodies (Sigma-Aldrich) were used. The membranes were then probed with HRP-conjugated secondary antibodies (Abcam, UK), and chemiluminescence was developed using the ECL solution (Millipore, USA). The signals were detected and analyzed using the Azure c300 chemiluminescent western blot imaging system (Azure Biosystems, USA).

Chromatin immunoprecipitation (ChIP) assay

The ChIP assay was performed using an ezChIP kit (Millipore) according to the manufacturer's instructions, using antibodies against c-Fos (#sc253), Runx2 (#sc-10758), or control IgG (#sc-2027) (Santa Cruz Biotechnology). The precipitated DNA samples were subjected to PCR amplification with the primers specific for the promoter region of NFATc1 containing an AP1 binding site or the primers specific for the ALP promoter region containing Runx2 binding sites. Real-time PCR was used to quantify ChIP assay results. All test Ct values were normalized by the input Ct value, and data represented as fold enrichment. The following primers were used for PCR and qPCR- NFATc1: forward, 5′-CCG GGA CGC CCA TGC AAT CTG TTA GTA ATT-3′; reverse, 5′-GCG GGT GCC CTG AGA AAG CTA CTC TCC CTT-3′; Alpl: forward, 5′-GGC TGG GAC AGA CAG AAT GT-3′; reverse, 5′-CTT TGT CCC TCG ATG GTT GT-3′.

Fractionation

Cultured cells were harvested after washing with ice-cold PBS and then cells were fractionated using NE-PER Nuclear and cytoplasmic Extraction Reagent (Thermo Fisher Scientific) according to the manufacturer's protocol. Cytoplasmic and nuclear extract were subjected to SDS-PAGE and Western blotting.

Microcomputed tomography (μCT) and histomorphometric analysis of bone loss model

For RANKL-induced bone loss models, 6-week-old male ICR mice were intraperitoneally injected with vehicle or GSK4112 (5 mg per kg of body weight; Sigma-Aldrich) on day 0. The mice were intraperitoneally injected with PBS or RANKL (1 mg/kg of body weight), and/or GSK4112 for the next 3 days and sacrificed on day five. For analyzing bone mass, mouse tibiae were fixed and scanned using a Skyscan 1172 system (Skyscan, Belgium) with the X-ray source at 50 kV and 201 μA and a 0.5 mm aluminum filter. The three-dimensional image obtained by CT-An (Skyscan), and three-dimensional morphometry was characterized by measuring the bone volume fraction (BV/TV), trabecular thickness (Tb.Th), trabecular separation (Tb.Sp), and trabecular number (Tb.N). The three-dimensional image of trabecular bone was remodeled using the ANT software (Skyscan). For bone histomorphometric analysis, tibiae were fixed in 4% paraformaldehyde and decalcified using 5.5% EDTA in 3.8% formaldehyde buffer for 2 weeks at 4°C. After the samples were gradually dehydrated and embedded in paraffin, the paraffin blocks were sectioned into 4 μm thick sections. H&E or TRAP staining was performed according to the standard protocol for determining osteoclasts and osteoblasts, respectively.

Statistical analysis

Unparied Student's *t*-test was calculated using IBM SPSS Statistics 21 (IBM, USA). The data were presented as mean ± SD. $P < 0.05$ was considered to be statistically significant.

RESULTS

Role of Rev-erbs in RANKL-induced osteoclast differentiation

We first examined the expression of Rev-erbα (also known as *Nr1d1*) and Rev-erbβ (also known as *Nr1d2*) during RANKL-induced osteoclast differentiation. When BMMs were cultured in the presence of M-CSF and RANKL, the expression of *Nfatc1* was gradually increased during osteoclast differentiation; the induction of *Nfatc1* was followed by the expression of *Oscar* and *Acp5*, which are osteoclast-specific genes. The mRNA expression of Rev-erbα and Rev-erbβ was gradually increased during osteoclast differentiation (Fig. 1A). Next, to investigate which Rev-erbs are more predominant in osteoclasts, we confirmed their role in osteoclast differentiation using Rev-erbα or Rev-erbβ specific siRNA. The expression of Rev-erbα and/or Rev-erbβ was significantly downregulated upon siRNA transfection in BMMs, as compared to control siRNA. Notably, the expression of Bmal1, a negative target gene of Rev-erb in the circadian pathway, was significantly enhanced by silencing of Rev-erbα or Rev-erbβ or both of the Rev-erbs (Fig. 1D, upper panel). RANKL treatment in the control siRNA-transfected BMMs increased the formation of osteoclast in a dose-dependent manner. The knockdown of Rev-erbα or Rev-erbβ slightly increased the osteoclast formation upon RANKL stimulation, as compared to control siRNA. Moreover, the knockdown of both Rev-erbs further enhanced the RANKL-induced osteoclast differentiation than knockdown of Rev-erbα or Rev-erbβ alone, as compared to control siRNA (Figs. 1B and 1C). Predictably, silencing of Rev-erbα or Rev-erbβ resulted in enhanced expression levels of osteoclast marker genes such as *Nfat1*, *Oscar*, *Acp5*, *Dcstamp,* and *Ctsk* in response to RANKL stimulation. Furthermore, silencing of both Rev-erbs strongly increased the mRNA expression of *Nfatc1*, *Oscar*, *Acp5*, *Dcstamp,* and *Ctsk* (Fig. 1D, lower panel). Overall, these results indicated that Rev-erbβ is functionally redundant to Rev-erbα with regard to the regulation of osteoclast differentiation.

Overexpression of Rev-erbs inhibits RANKL-induced osteoclast differentiation

Given our data indicating the effect of Rev-erbs on osteoclast differentiation by performing loss-of-function experiments, we overexpressed Rev-erbα or Rev-erbβ to confirm their role in osteoclasts through gain-of-function experiments.

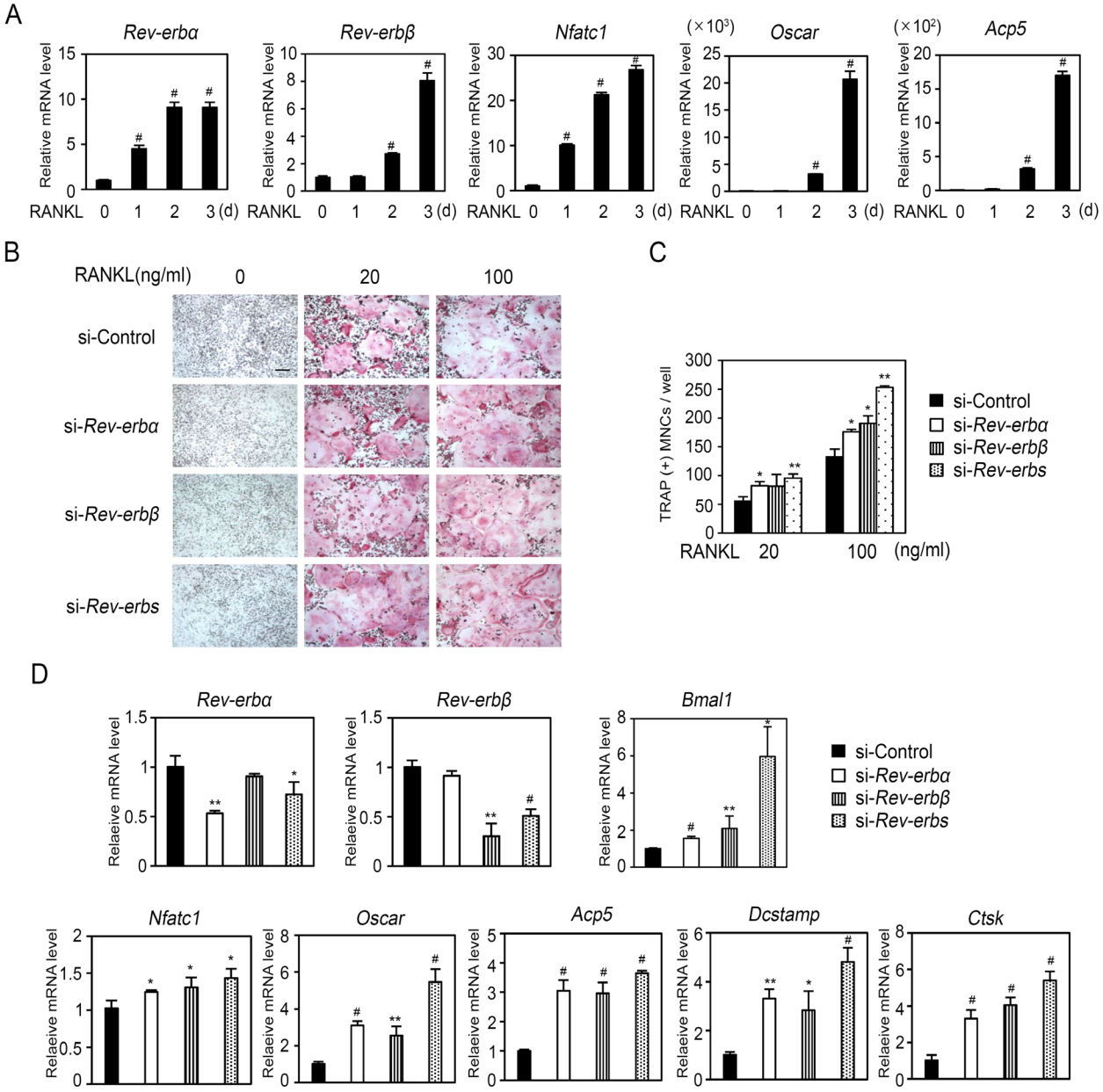

Fig. 1. Expression of Rev-erbs and effect of knockdown of Rev-erbα and Rev-erbβ in RANKL-induced osteoclast formation. (A) BMMs were cultured with M-CSF (30 ng/ml) and RANKL (100 ng/ml) for the indicated times. Total RNA was isolated from the cell lysates and mRNA expression of *Rev-erbα*, *Rev-erbβ*, *Nfatc1*, *Oscar*, and *Acp5* was assessed by real-time PCR. The values shown are normalized to GAPDH levels. The data represent mean ± SD of triplicate samples. $^{\#}P < 0.005$ vs 0 day. (B-D) BMMs were transfected with control siRNA (si-Control) or siRNA specific for Rev-erbα (si-*Rev-erbα*), Rev-erbβ (si-*Rev-erbβ*), and both Rev-erbα and Rev-erbβ (si-*Rev-erbs*). (B) Transfected BMMs were cultured for 3 days with M-CSF and various concentrations of RANKL, as indicated. The cultured cells were fixed and stained for TRAP. Scale bars = 100 μm. (C) The numbers of TRAP(+)MNCs were counted. The data represent means ± SD of triplicate samples. $*P < 0.05$, $**P < 0.01$ vs control siRNA. The results shown are representative of at least three independent sets of similar experiments. (D) Transfected BMMs were cultured with M-CSF and RANKL for 3 days. Relative mRNA expression was determined by real-time PCR. The data represent means ± SD of triplicate samples. $*P < 0.05$, $**P < 0.01$, $^{\#}P < 0.005$ vs si-Control.

The formation of osteoclasts was increased with RANKL administration in a dose-dependent manner in BMMs infected with control vector. However, RANKL-induced osteoclast formation was significantly inhibited in BMMs overexpressing Rev-erbα (Figs. 2A and 2B). In addition, overexpression of Rev-erbα strongly attenuated RANKL-mediated induction of *Nfatc1*, *Oscar*, and *Acp5*, indicating that Rev-erbα affects the expression of osteoclast markers at the mRNA level during

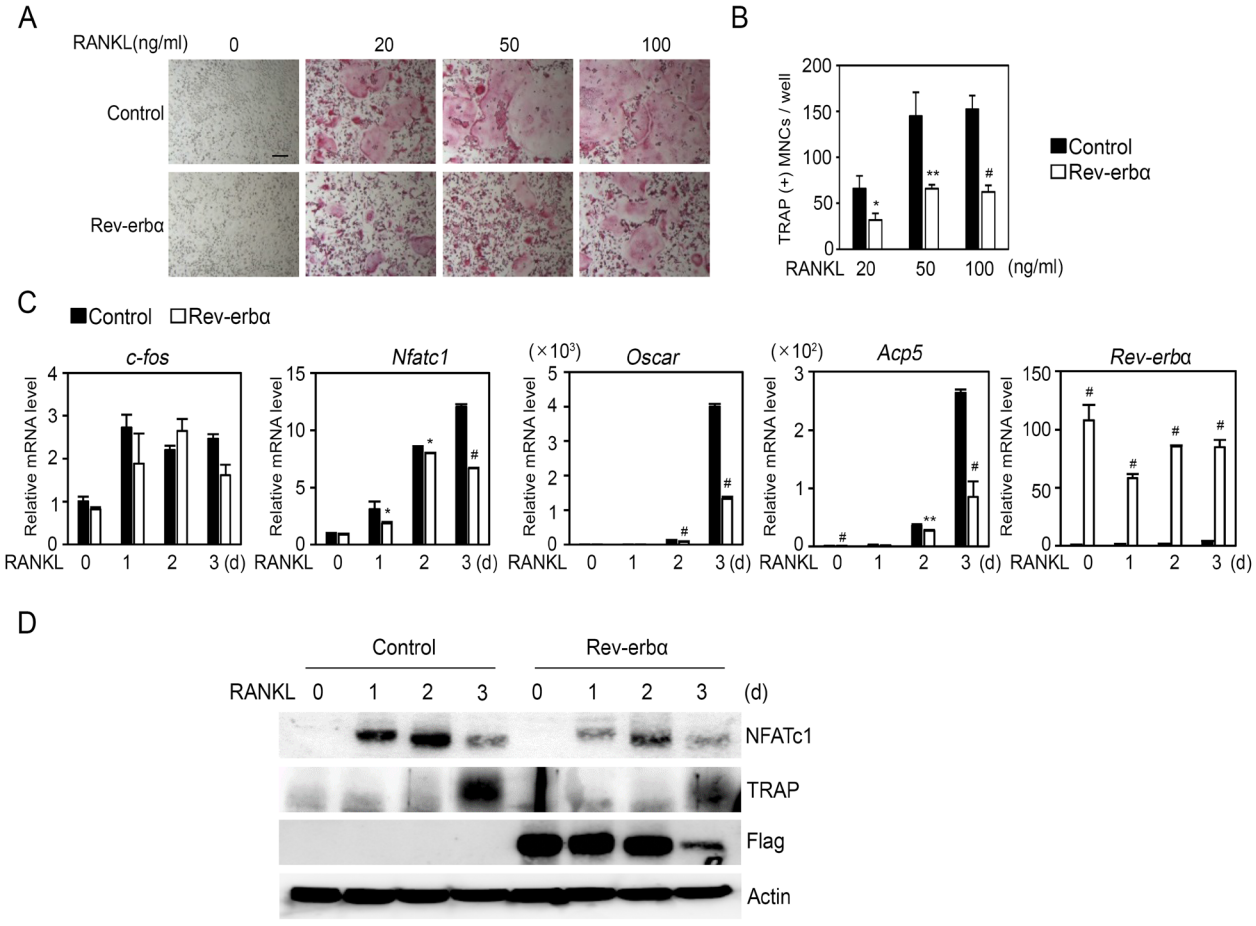

Fig. 2. Overexpression of Rev-erbα inhibits RANKL-induced osteoclast differentiation. BMMs were infected with either pMX-IRES-EGFP (Control) or Rev-erbα retroviruses. The transduced BMMs were cultured with M-CSF and various concentrations of RANKL for the indicated times. (A) Cells cultured for 3 days were fixed and stained for TRAP. Scale bars = 100 μm. (B) The numbers of TRAP(+)MNCs per well were counted. $*P < 0.05$, $**P < 0.01$, $^{\#}P < 0.005$ vs control. (C) Real-time PCR was performed to determine mRNA expression of *c-Fos*, *Nfatc1*, *Oscar*, *Acp5*, and *Rev-erbα*. The data represent mean ± SD of triplicate samples. $*P < 0.05$, $**P < 0.01$, $^{\#}P < 0.005$ vs control. (D) Cells from each time point were harvested, and the lysates were analyzed by western blot with specific antibodies, as indicated.

osteoclast differentiation with the exception of *c-Fos* (Fig. 2C). Rev-erbα attenuated the protein expression of NFATc1 and TRAP during osteoclastogenesis (Fig. 2D). Since the downregulation of Rev-erbβ enhanced the RANKL-induced osteoclast differentiation, we investigated the role of Rev-erbβ by retroviral-mediated overexpression in BMMs. The overexpression of Rev-erbβ in BMMs significantly inhibited the RANKL-induced osteoclast formation as compared to the control (Supplementary Figs. S1A and S1B). Moreover, the overexpression of Rev-erbβ greatly inhibited the expression of *Nfatc1*, *Oscar*, and *Acp5* (Supplementary Fig. S1C). Taken together, these results suggested that Rev-erbα and Rev-erbβ negatively regulate RANKL-induced osteoclast differentiation.

Rev-erbα targets NFATc1 on osteoclasts

It has been established that RANKL strongly stimulates c-Fos induction, and then the binding of c-Fos to NFATc1 promoter induces NFATc1 gene expression at an early stage of osteoclast differentiation (Kim and Kim, 2016). In order to further clarify the molecular mechanism by which Rev-erbα regulates NFATc1 expression in RANKL-induced osteoclast differentiation, we examined whether Rev-erbα can interact with NFATc1. Rev-erbα did not interact with NFATc1 (Supplementary Fig. S2). To examine the effects of Rev-erbα in c-Fos-dependent NFATc1 induction, 293T cells were transfected with NFATc1 reporter plasmid containing a 6.2-kb NFATc1 promoter and c-Fos, with or without Rev-erbα. c-Fos significantly induced the transcriptional activity of NFATc1 while addition of Rev-erbα strongly inhibited this activation in a dose dependent manner (Fig. 3A). Next, since Rev-erbα prevented c-Fos-induced NFATc1 expression, we examined whether Rev-erbα can interact with c-Fos. As shown in Figure 3B, Rev-erbα interacted with c-Fos. In addition, ChIP assay showed that Rev-erbα inhibited binding of c-Fos to the NFATc1 promoter region in osteoclasts (Figs. 3C and 3D). Taken together, these results demonstrated that Rev-erbα

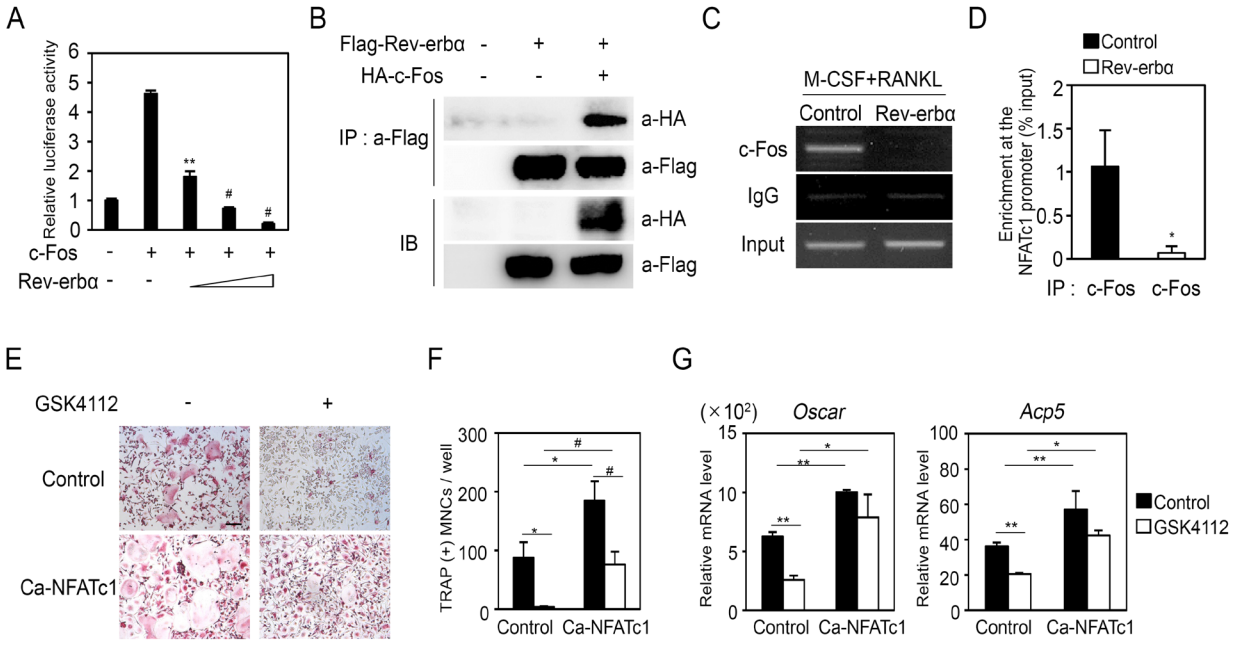

Fig. 3. The effect of Rev-erbα on NFATc1 expression. (A) 293T cells were co-transfected with the NFATc1 luciferase reporter and c-Fos, as well as increasing concentrations of Rev-erbα. After 36 h of transfection, the cells were lysed, and their luciferase activity was determined. The data represent mean ± SD of triplicate samples. $^{**}P < 0.01$, $^{\#}P < 0.005$ vs control. (B) 293T cells were co-transfected with Flag-Rev-erbα and HA-c-Fos. Cell lysates were harvested and immunoprecipitated with an anti-Flag antibody. The immunoprecipitated samples and whole cell lysates were subjected to SDS-PAGE and Western blotting using an anti-HA or anti-Flag antibody. (C and D) BMMs transduced with pMX-IRES-EGFP (Control) or Rev-erbα retroviruses were cultured with M-CSF and RANKL for 1 day. After crosslinking, the samples were immunoprecipitated with control IgG or anti-c-Fos and subjected to real-time PCR with primers specific to the NFATc1 promoter region containing AP1-binding sites. The data represent mean ± SD of triplicate samples. $^{*}P < 0.05$ vs control. (E) BMMs were infected with either MSCV (Control) or Ca-NFATc1 retroviruses. The transduced BMMs were cultured with M-CSF and RANKL, with or without GSK4112, for 3 days, and the cells were then fixed and stained for TRAP. Scale bars = 100 μm. (F) The numbers of TRAP(+) MNCs per well were counted. The data represent mean ± SD of triplicate samples. $^{*}P < 0.05$, $^{\#}P < 0.005$ vs control. (G) Real-time PCR was performed to determine mRNA expression of *Oscar* and *Acp5*. The data represent mean ± SD of triplicate samples. $^{*}P < 0.05$, $^{**}P < 0.01$, $^{\#}P < 0.005$ vs control.

competes with c-Fos recruitment to attenuate NFATc1 induction. To investigate whether the inhibitory effect of Rev-erbα on osteoclast formation could be rescued by overexpression of NFATc1, a constitutively active form of NFATc1 (Ca-NFATc1) was overexpressed in BMMs. GSK4112, a synthetic Rev-erb agonist, binds directly to the ligand binding domain of Rev-erbs (Trump et al., 2013). Treatment with GSK4112 strongly prevented formation of TRAP-positive multinucleated cells in a dose dependent manner (Supplementary Figs. S3A and S3B). To clarify the possibility that anti-osteoclastogenic activity of GSK4112 could be due to its cytotoxicity in BMMs, we investigated the cytotoxic effect of GSK4112 in BMMs. GSK4112 exhibited significant cytotoxicity at concentration above 30 nM (Supplementary Fig. S3C), suggesting that anti-osteoclastogenic activity of GSK4112 without any cytotoxicity could be expected under 20 nM. Additionally, the inhibitory effect of GSK4112 on osteoclast differentiation was evaluated by mRNA expression levels of osteoclast-specific genes. GSK4112 strongly attenuated the RANKL-mediated induction of *Nfatc1*, *Oscar,* and *Acp5* during osteoclast differentiation with the exception of *c-Fos* (Supplementary Fig. S3D). GSK4112 strongly blocked the osteoclast formation, while overexpression of Ca-NFATc1 significantly blocked the GSK4112-mediated downregulation of RANKL-induced osteoclast formation (Figs. 3E and 3F). GSK4112-mediated downregulation of *Oscar* and *Acp5* was reversed by overexpression Ca-NFATc1 (Fig. 3G). Taken together, these results indicated that Rev-erbα targets NFATc1 and regulates c-Fos-induced NFATc1 expression in osteoclasts.

Knockdown of Rev-erbα enhances osteoblast differentiation

Rev-erbα could promote bone marrow stromal cells (BMSC) aging and may act as a negative regulator during the late phase of osteogenesis (He et al., 2015). However, the mechanism of Rev-erbα and Rev-erbβ in osteoblasts remains yet unknown. In order to examine the expression of Rev-erbα and Rev-erbβ during osteoblast differentiation, bone marrow-derived stromal cells were cultured with ascorbic acid, β-glycerophosphate, and IGF-1. The expression of osteogenic genes including alkaline phosphatase (*Alpl*), bone sialoprotein (*Ibsp*), and osteocalcin (*Bglap*) was significantly increased

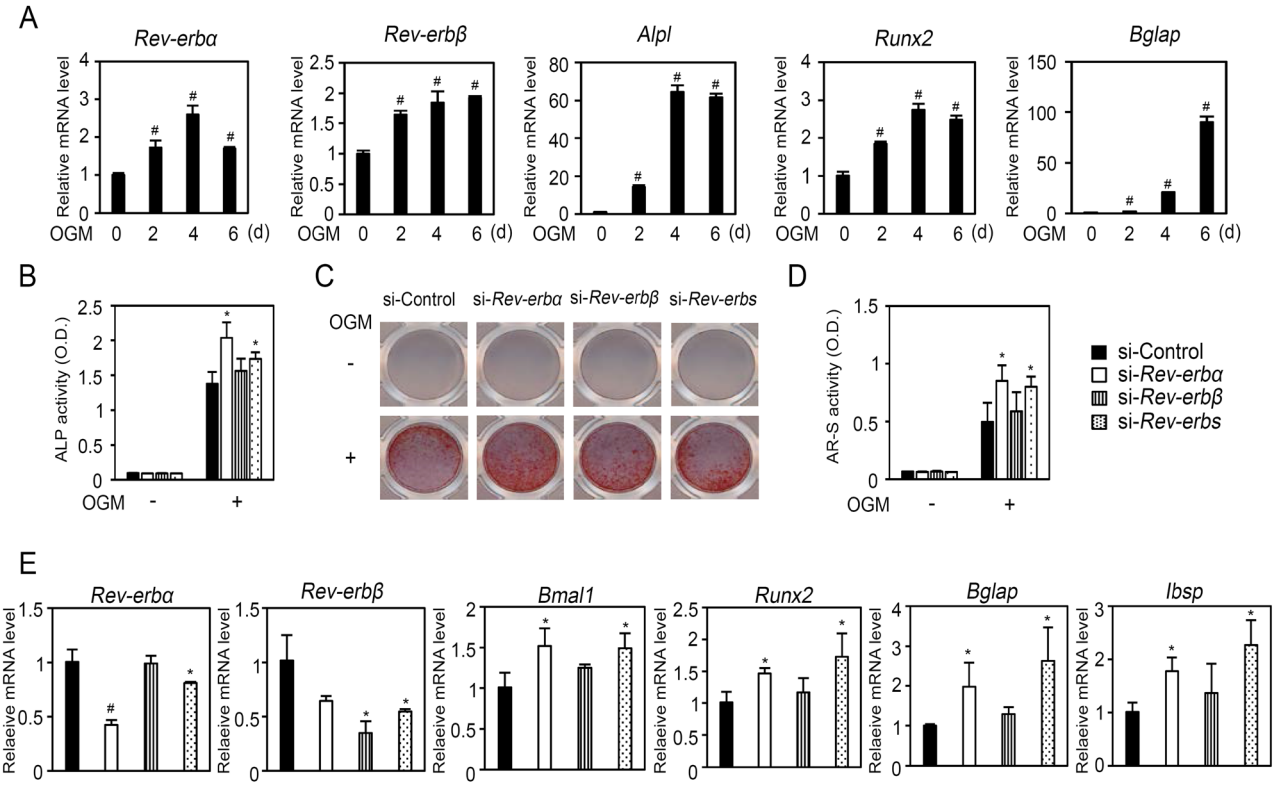

Fig. 4. Expression of Rev-erbs during osteoblast differentiation and their effect on osteoblast differentiation. BMSCs were incubated with osteogenic medium containing IGF-1 (50 ng/ml), ascorbic acid (50 μg/ml), and β-glycerophosphate (100 μM) for the indicated times. (A) Total RNA was isolated from the cell lysates and real-time PCR was performed to determine mRNA expression of *Rev-erbα*, *Rev-erbβ*, *Alpl*, *Runx2*, and *Bglap*. The data represent mean ± SD of triplicate samples. The values shown are normalized to GAPDH levels. $^{\#}P < 0.005$ vs day 0. (B-E) BMSCs were transfected with control siRNA (si-Control) or siRNA specific for Rev-erbα (si-*Rev-erbα*), Rev-erbβ (si-*Rev-erbβ*), and both Rev-erbα and Rev-erbβ (si-*Rev-erbs*). (B) Cells were cultured for 4 days, and ALP activities were measured by densitometry at 405 nm. O.D., optical density. The data represent mean ± SD of triplicate samples. $*P < 0.05$ vs control siRNA. (C) Cells cultured for 9 days were fixed and stained with alizarin red. (D) Alizarin red staining activity was quantified by densitometry at 570 nm. The data represent mean ± SD of triplicate samples. $*P < 0.05$ vs control siRNA. (E) Transfected cells were cultured with osteogenic medium containing IGF-1, ascorbic acid, and β-glycerophosphate for 6 days. Total RNA was isolated from the cell lysates and mRNA expression of *Rev-erbα*, *Rev-erbβ*, *Bmal1*, *Runx2*, *Bglap*, and *Ibsp* were assessed by real-time PCR. The values shown are normalized to GAPDH levels. The data represent mean ± SD of triplicate samples. $*P < 0.05$ vs si-Control.

during osteoblast differentiation, and the expression of Rev-erbα and Rev-erbβ was also increased during differentiation (Fig. 4A). We examined the physiological roles of Rev-erbs in osteoblast differentiation using specific siRNA of Rev-erbα or Rev-erbβ. The expression of Rev-erbα, Rev-erbβ, or both Rev-erbs was significantly downregulated by Rev-erbα- and Rev-erbβ-specific siRNA, as compared to control siRNA, respectively. The knockdown of Rev-erbα but not Rev-erbβ, in osteoblasts, significantly increased the expression of Bmal1 in particular (Fig. 4E). Next, ALP activity and bone nodule formation were evaluated as markers of osteoblast differentiation and function. Rev-erbα siRNA and siRNA against both Rev-erbs significantly increased the ALP activity and mineralized nodule formation; however, Rev-erbβ siRNA did not affect osteoblast differentiation and function. (Figs. 4B-4D). These results indicated that Rev-erbβ is not functionally redundant to Rev-erbα in osteoblast differentiation. Moreover, knockdown of Rev-erbα and both the Rev-erbs significantly increased the expression of *Runx2*, *Bglap*, and *Ibsp* during osteoblast differentiation (Fig. 4E). Collectively, these results suggest that Rev-erbα plays a dominant role in osteoblast differentiation and function.

Overexpression of Rev-erbα attenuates osteoblast differentiation and function

Next, we examined the effect of Rev-erbα overexpression in osteoblasts. Overexpression of Rev-erbα in preosteoblasts strongly inhibited ALP activity, mineralized nodule formation, and alizarin red activity under the osteogenic conditions (Figs. 5A-5C). Moreover, Rev-erbα overexpression significantly attenuated the expression of *Runx2*, *Alpl*, *Bglap*, and *Ibsp* during osteoblast differentiation as compared to overexpression of control vector (Fig. 5D). To determine the impact of Rev-erbα on Runx2 activity in osteoblasts, we investigated nuclear translocation of Runx2, a requisite event in its transcriptional activity. Overexpression of Rev-erbα suppressed

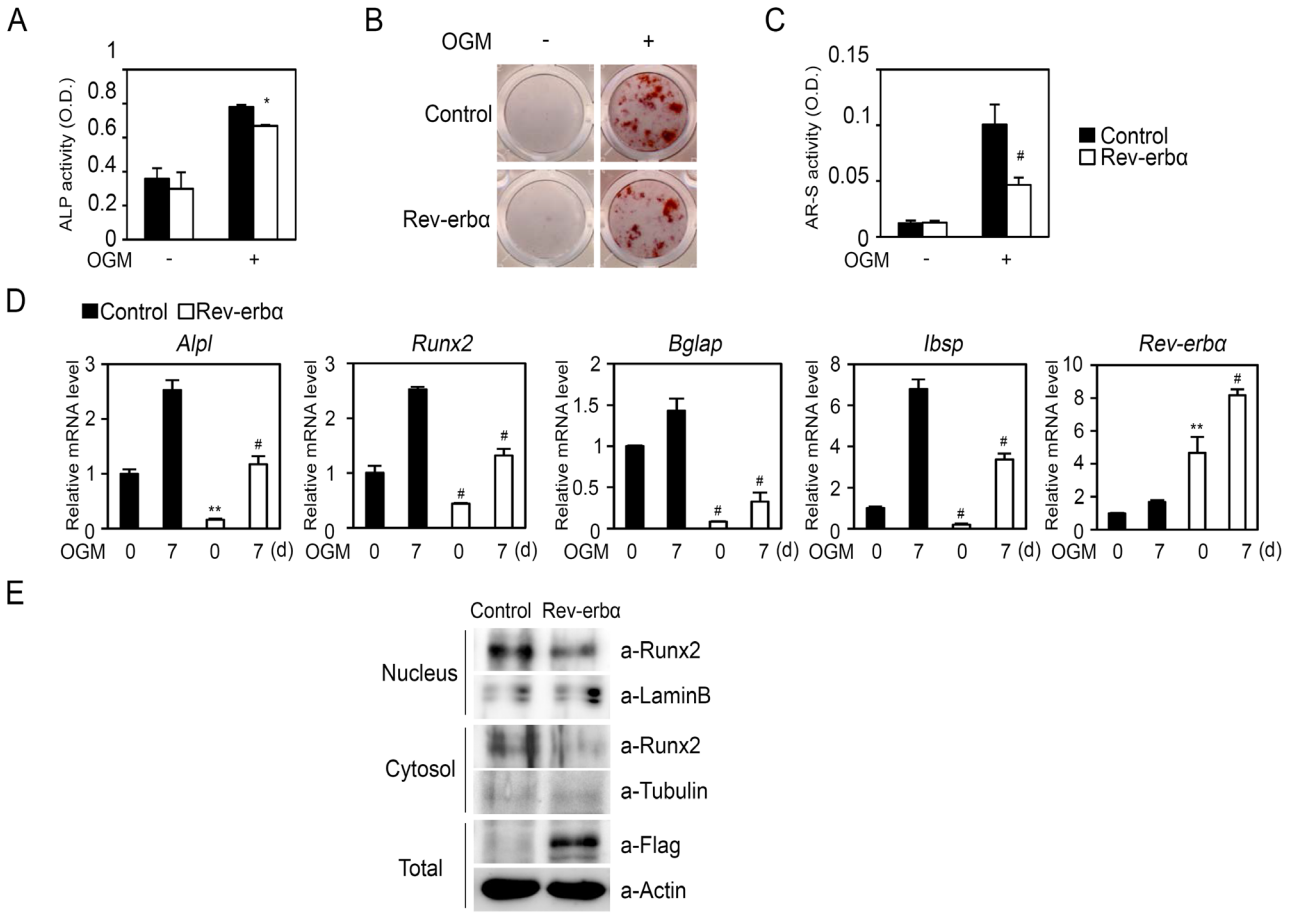

Fig. 5. Rev-erbα overexpression inhibits osteoblast differentiation via regulation of Runx2 nuclear translocation. BMSCs were transduced with either pMX-IRES-EGFP (control) or Rev-erbα retroviruses, and cultured with osteogenic medium containing IGF-1, ascorbic acid, and β-glycerophosphate. (A) Cells were cultured for 4 days, and ALP activities were measured by densitometry at 405 nm. O.D., optical density. The data represent mean ± SD of triplicate samples. $*P < 0.05$ vs control. (B) Cells were cultured for 9 days, and were fixed and stained for alizarin red. (C) Alizarin red staining activity was quantified by densitometry at 570 nm. The data represent mean ± SD of triplicate samples. $^{\#}P < 0.005$ vs control. (D) Real-time PCR was performed to determine mRNA expression of *Alpl*, *Runx2*, *Bglap*, *Ibsp*, and *Rev-erbα*. The data represent mean ± SD of triplicate samples. $**P < 0.01$, $^{\#}P < 0.005$ vs control. (E) BMSCs were transduced with either pMX-IRES-EGFP (control) or Rev-erbα retroviruses, and cultured with osteogenic medium containing IGF-1, ascorbic acid, and β-glycerophosphate for 6 days. Whole cell extracts, cytoplasmic fractions, and nuclear fractions were harvested from the cultured cells and subjected to western blot analysis with specific antibodies as indicated. Antibodies for tubulin and LaminB1 were used for the normalization of cytoplasmic and nuclear extracts, respectively.

Runx2 nuclear translocation as compared to overexpression of control vector (Fig. 5E). Taken together, these results suggest that Rev-erbα negatively regulates osteoblast differentiation and function.

Rev-erbα modulates Runx2 activity in osteoblasts

Since it has been previously reported that osteoblast-related genes such as type I collagen and Runx2 are involved in circadian rhythms *in vivo* (Fujihara et al., 2014), we investigated the effect of Rev-erbα on transcriptional regulation of Runx2. Rev-erbα significantly repressed luciferase activity of the Runx2-responsive osteocalcin reporter 6XOSE2, induced by Runx2 (Fig. 6A). Co-immunoprecipitation experiment showed that Rev-erbα associated with Runx2 (Fig. 6B). To determine whether Rev-erbα affected the binding of Runx2 to its target promoter region in vivo, ChIP assay was performed using cultured mature osteoblasts. Rev-erbα reduced the recruitment of Runx2 to the promoter region of ALP and BSP (Figs. 6C-6F). Taken together, these results suggest that Rev-erbα negatively regulates osteoblast differentiation via regulation of Runx2.

Rev-erbα regulates p38 MAPK signaling in both osteoclasts and osteoblasts

Next, we investigated the effect of Rev-erbα on intracellular signaling pathways involved in osteoclasts and osteoblasts. RANKL induced the activation of p38 MAPK, JNK, and ERK and degradation of IκBα in control vector-infected BMMs.

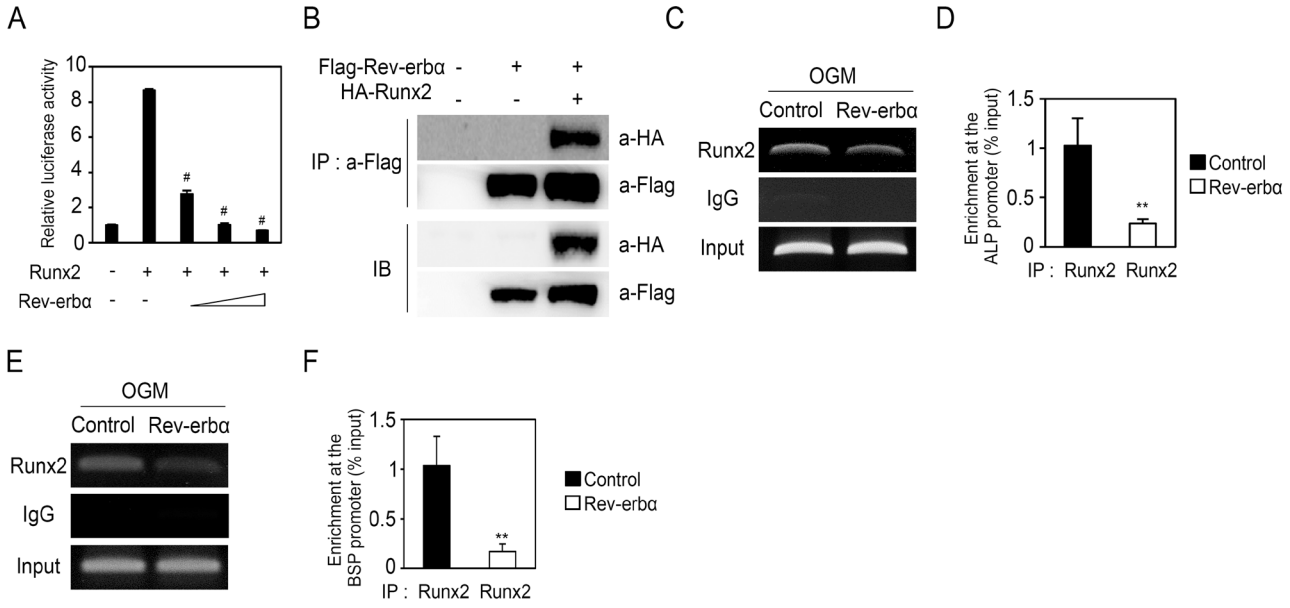

Fig. 6. Rev-erbα interacts with Runx2 and inhibits recruitment of Runx2 to the ALP promoter and BSP promoter. (A) 293T cells were co-transfected with 6XOSE luciferase reporter and Runx2 along with increasing concentrations of Rev-erbα. After 36 h of transfection, the cells were assayed for relative luciferase activity. The data represent mean ± SD of triplicate samples. $^{\#}P < 0.005$ vs control. (B) 293T cells were co-transfected with Flag-Rev-erbA and HA-Runx2. The cell lysates were harvested and immunoprecipitated with an anti-Flag antibody. The immunoprecipitated samples and whole cell lysates were subjected to SDS-PAGE and Western blotting using an anti-HA or anti-Flag antibody. (C-F) BMSCs were transduced with either pMX-IRES-EGFP (control) or Rev-erbα retroviruses, and were cultured with osteogenic medium for 9 days. After crosslinking, the samples were immunoprecipitated with control IgG or anti-Runx2 and subjected to real-time PCR with primers specific to the ALP promoter (C and D), and BSP promoter (E and F) containing Runx2-binding sites. The data represent mean ± SD of triplicate samples. $^{**}P < 0.01$ vs control.

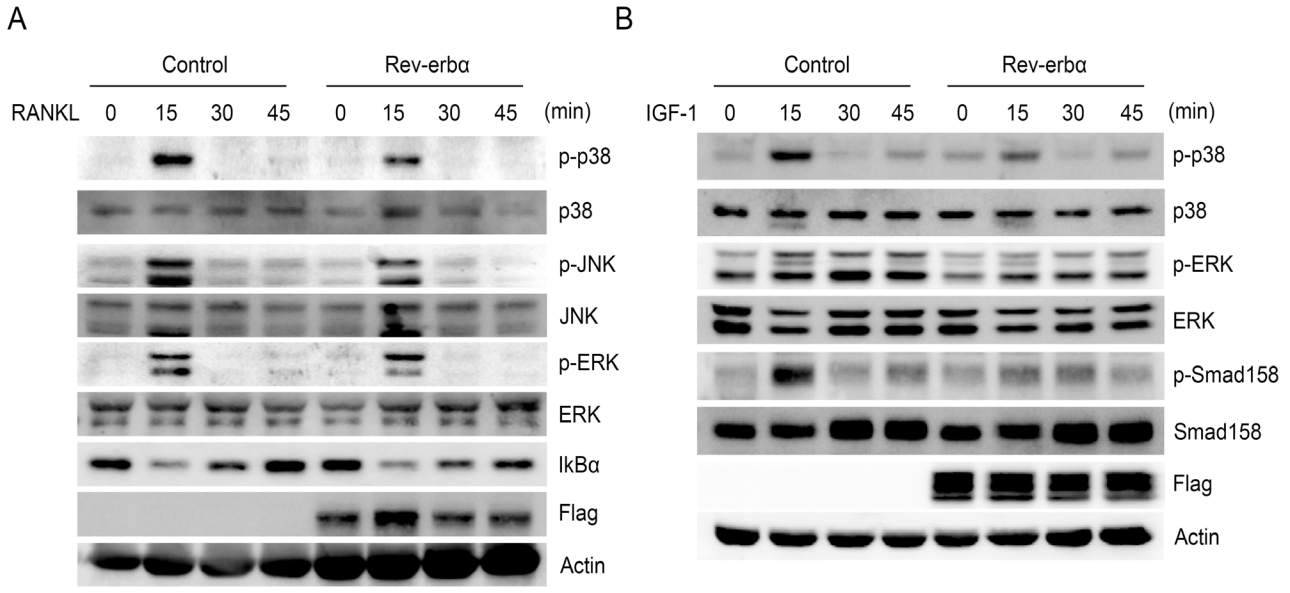

Fig. 7. Rev-erbα inhibits p38 MAPK signaling in osteoclasts and osteoblasts. (A) BMMs were transduced with pMX-IRES-EGFP (control) or Rev-erbα retroviruses, and were stimulated with RANKL for the indicated times. (B) BMSCs were transduced with either pMX-IRES-EGFP (control) or Rev-erbα retroviruses, and were stimulated with IGF-1 for the indicated times. (A and B) Whole cell lysates were subjected to western blot analysis with specific antibodies, as indicated.

RANKL-induced phosphorylation of p38 MAPK and JNK was attenuated by Rev-erbα overexpression as compared to the control. On the other hand, IκBα degradation and ERK phosphorylation were unaffected (Fig. 7A). IGF-1 induced signaling pathways such as MAPK, ERK, and Smad in osteoblasts. The overexpression of Rev-erbα inhibited p38 MAPK, ERK, and Smad phosphorylation as compared to the overexpression of control vector (Fig. 7B). These data suggested that Rev-erbα might commonly regulate p38 MAPK in both osteoclasts and osteoblasts.

GSK4112 blocks RANKL-induced bone loss *in vivo*

In order to investigate it as a therapeutic target of Rev-erb in bone diseases, we tested GSK4112 using RANKL-induced bone loss model. RANKL or PBS together with GSK4112 was intraperitoneally injected into the mice. μCT analysis with three-dimensional reconstruction of trabecular bone revealed that injection of RANKL markedly decreased the bone mass as compared to the control group; however, intraperitoneal administration of GSK4112 prevented the RANKL-induced bone loss (Fig. 8A). Further, osteoporotic phenotype due to RANKL-induced bone loss was determined quantitatively by measuring the decrease in the percent of bone volume to total tissue volume and trabecular numbers, as well as the accompanied increase of trabecular separation and thickness as compared to control group, whereas the administration

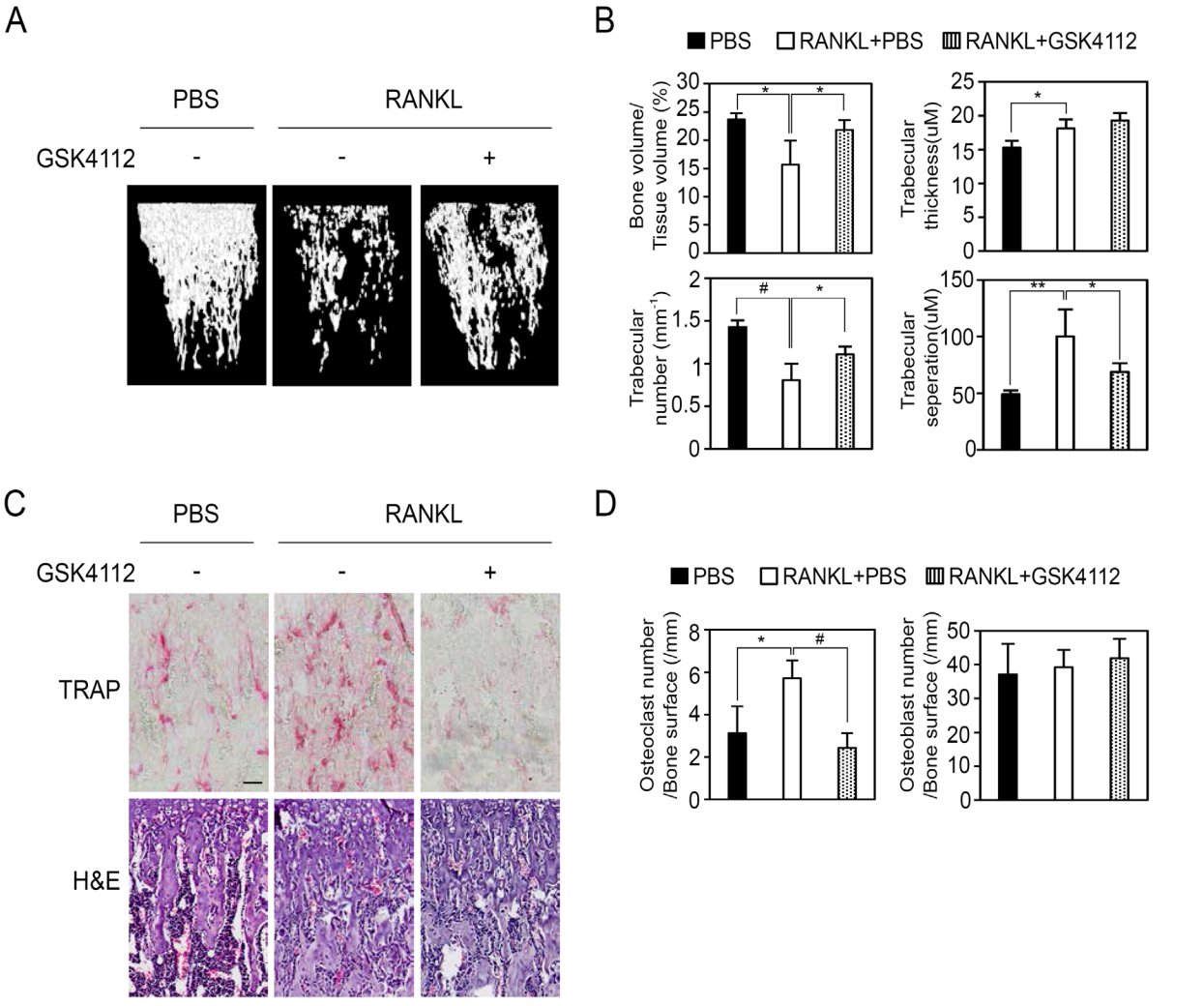

Fig. 8. Administration of GSK4112 prevents RANKL-induced bone loss in mice. Mice were intraperitoneally administrated with PBS, RANKL, with or without GSK4112. The long bones obtained from mice were subjected to μCT and immunohistochemical analysis. (A) Representative three-dimensional images of femoral metaphysis from PBS-, RANKL-, and RANKL plus GSK4112-injected mice. (B) Bone volume per tissue volume (BV/TV), trabecular thickness (Tb.Th), trabecular separation (Tb.Sp), and trabecular number (Tb.N) were assessed from the μCT measurements. The data represent mean ± SD. $*P < 0.05$, $**P < 0.01$, $^{\#}P < 0.005$ vs PBS. (C) H&E staining and TRAP staining of histological sections of proximal tibiae. Scale bars = 100 μm. (D) Osteoclast surface per bone surface, osteoclast number per bone surface, osteoblast surface per bone surface, and osteoblast number per bone surface were assessed. The data are represented as the mean ± SD. $*P < 0.05$, $^{\#}P < 0.005$ vs PBS.

of GSK4112 obviously suppressed RANKL-induced bone destruction (Fig. 8B). Next, to confirm bone loss recovery by GSK4112 administration at the cellular level in trabecular bones of the proximal tibia of mice, immunohistochemistry analysis was performed for quantification using TRAP and H&E staining, respectively. After RANKL injection, there was an increase in the number of TRAP-positive osteoclasts, while osteoclast number was significantly decreased in trabecular bones of mouse injected with GSK4112. However, the number of osteoblasts in trabecular bone remained unchanged between RANKL and GSK4112 administration, demonstrating that reduction of bone loss by GSK4112 was due to inhibition of osteoclast formation *in vivo* (Figs. 8C and 8D). Therefore, these results suggest that Rev-erb agonist may be useful for the treatment of bone disease characterized by excessive bone resorption.

DISCUSSION

Bone homeostasis is maintained via the balance between bone resorption and bone formation by osteoclasts and osteoblasts. Since the two processes are closely related, it is necessary to develop therapeutic agents that are able to inhibit bone resorption and promote bone formation in bone diseases such as osteoporosis.

Recently, it was reported that the circadian clock controls many aspects of energy metabolism, the immune system, and cardiovascular physiology (Maury et al., 2014). It has been reported that circadian rhythms are identified in bone and that the clock and clock control genes in the bones are crucial to bone metabolism (Iimura et al., 2012). Osteoclasts and osteoblasts have been shown to express clock genes associated with the circadian signaling pathway and exhibit circadian rhythmicity controlled by various endocrine hormones and cytokines (Fujihara et al., 2014; McElderry et al., 2013).

In this study, we revealed that Rev-erbα acts as a negative regulator in osteoclasts and osteoblasts. The overexpression of Rev-erbα and Rev-erbβ showed anti-osteoclastogenic activity through regulation of p38 MAPK activation and NFATc1 expression. Conversely, knockdown of Rev-erbα and Rev-erbβ in BMMs, by small interfering RNA, showed the opposite effects. In addition, administration of GSK4112, a Rev-erb agonist, prevented RANKL-induced bone destruction by attenuating osteoclast formation, suggesting that Rev-erb agonist may be beneficial as therapeutic target for bone diseases such as osteoporosis. Consistent with our results, it has been reported that SR9009, a structurally distinct Rev-erb agonist, inhibited osteoclast differentiation, and the pharmacologic activation of SR9009 has been reported to improve ovariectomy-induced bone loss (Song et al., 2018).

Our study revealed that Rev-erbα knockdown significantly enhanced osteoblast differentiation, while overexpression of Rev-erbα attenuated osteoblast differentiation and function, and inhibited Runx2 activity via p38 MAPK signaling pathway. However, downregulation of Rev-erbβ did not affect osteoblast differentiation, suggesting that Rev-erbα plays a predominant role in osteoblasts. Accumulating studies have focused on the relationship between Rev-erbα and adipogenesis, while little is known about mechanism of Rev-erbα in osteogenesis (Fontaine et al., 2003). According to a recent report, Rev-erbα expression is declined during BMSC-induced osteoblast differentiation and Rev-erbα promotes BMSC aging, suggesting that Rev-erbα may be a negative regulator during the late phase of osteogenesis (He et al., 2015). These results are partly consistent with our results that overexpression of Rev-erbα inhibits BMSC-induced osteoblast differentiation. Unlike the reported results, we showed that the expression of Rev-erbα was induced by osteogenic factors in the BMSCs (Fig. 4). These discrepancies may be possibly because of the difference in the cell culture method such as cell source, and/or cell density, and/or cell differentiation factor in given cell culture conditions.

Interestingly, it has been reported that circadian rhythms are prevalent in bone metabolism. Indeed, the transcription factor BMAL1, controlled by Rev-erb, plays a role in the circadian clock by adjusting the balance between bone formation and bone resorption, which is important for bone homeostasis (Li et al., 2018; Samsa et al., 2016; Xu et al., 2016). Moreover, osteoclast-related genes such as CTSK and NFATc1, but not another marker TRAP showed circadian rhythmicity in the femur of mice. In addition, osteoblast-related genes such as type I collagen and Runx2 in calvarial bone showed circadian variation (Fujihara et al., 2014; Zvonic et al., 2007). Rev-erbα and Rev-erbβ have been characterized as potent transcriptional factors that repress recruitment of the corepressor molecules such as NCoR and HDAC3 to the target gene promoters involved in the circadian cycle (Lazar, 2016; Yin and Lazar, 2005). According to recent studies, NCoR inhibits the binding of c-Jun/c-Fos hetero dimer to an AP-1 target gene involved in inflammatory responses (Ogawa et al., 2004) and HDAC3 interacts with Runx2 to repress the osteocalcin promoter (Schroeder et al., 2004). These data support our results that Rev-erbα results in the transcriptional repression of genes involved in the circadian rhythm such as NFATc1 and Runx2. It is thought that Rev-erb is accompanied by co-repressors and represses target gene transcription, leading to histone modification of critical circadian genes.

In the present study, we found that Rev-erbα not only attenuated the RANKL-induced phosphorylation of p38 MAPK in BMMs, but also inhibited the IGF-induced p38 MAPK phosphorylation in BMSCs. Indeed, p38 MAPK has been known to play a critical role in skeletal development and bone homeostasis. In osteoclasts, it has been shown that activated p38 MAPK can trigger translocation of NFATc1 to nuclei via phosphorylation followed by formation of a complex of NFATc1/PU.1 in response to RANKL, so as to increase CTSK and TRAP gene expression (Bohm et al., 2009; Matsumoto et al., 2004). Moreover, p38 MAPK has been identified as a positive regulator of osteoblast differentiation and function, in part by regulating the transcription activity of Runx2 (Greenblatt et al., 2010). Taken together, our results suggest that Rev-erbα negatively regulates bone remodeling by inhibiting p38 MAPK signaling pathways that consequently downregulate the expression and activity of NFATc1 and Runx2 in osteoclasts and osteoblasts, respectively.

Rev-erbα acts in a tissue-specific manner to regulate circadian rhythms and metabolism and in some cases exhibits redundant functions with Rev-erbβ (Lazar, 2016). Intriguingly,

we observed that Rev-erbα and Rev-erbβ regulate osteoclast differentiation, but Rev-erbβ did not participate in osteoblast differentiation despite it being present during the differentiation process. These data suggest that Rev-erbα and Rev-erbβ have distinct roles in both the bone cells.

Collectively, we demonstrated that Rev-erbα acts as a negative regulator in osteoclasts and osteoblasts. Further, our finding suggests that development of dissociated synthetic pharmacological agonist of Rev-erbs can serve as an approach for therapeutic treatment of bone disease characterized by excessive bone resorption.

Note: Supplementary information is available on the Molecules and Cells website (www.molcells.org).

Disclosure
The authors have no potential conflicts of interest to disclose.

ACKNOWLEDGMENTS
This work was supported by the National Research Foundation of Korea (NRF) grants funded by the Korea government (MIST) (No. 2019R1A5A2027521 and 2017R1A2B2005417).

ORCID
Kabsun Kim https://orcid.org/0000-0002-8320-5030
Jung Ha Kim https://orcid.org/0000-0003-2543-043X
Inyoung Kim https://orcid.org/0000-0001-9749-1499
Semun Seong https://orcid.org/0000-0002-6631-7129
Nacksung Kim https://orcid.org/0000-0002-8132-3981

REFERENCES
Bohm, C., Hayer, S., Kilian, A., Zaiss, M.M., Finger, S., Hess, A., Engelke, K., Kollias, G., Kronke, G., Zwerina, J., et al. (2009). The alpha-isoform of p38 MAPK specifically regulates arthritic bone loss. J. Immunol. *183*, 5938-5947.

Cao, X. and Chen, D. (2005). The BMP signaling and in vivo bone formation. Gene *357*, 1-8.

Day, T.F., Guo, X., Garrett-Beal, L., and Yang, Y. (2005). Wnt/beta-catenin signaling in mesenchymal progenitors controls osteoblast and chondrocyte differentiation during vertebrate skeletogenesis. Dev. Cell *8*, 739-750.

Duez, H. and Staels, B. (2009). Rev-erb-alpha: an integrator of circadian rhythms and metabolism. J. Appl. Physiol. (1985) *107*, 1972-1980.

Fontaine, C., Dubois, G., Duguay, Y., Helledie, T., Vu-Dac, N., Gervois, P., Soncin, F., Mandrup, S., Fruchart, J.C., Fruchart-Najib, J., et al. (2003). The orphan nuclear receptor Rev-erbalpha is a peroxisome proliferator-activated receptor (PPAR) gamma target gene and promotes PPARgamma-induced adipocyte differentiation. J. Biol. Chem. *278*, 37672-37680.

Fujihara, Y., Kondo, H., Noguchi, T., and Togari, A. (2014). Glucocorticoids mediate circadian timing in peripheral osteoclasts resulting in the circadian expression rhythm of osteoclast-related genes. Bone *61*, 1-9.

Greenblatt, M.B., Shim, J.H., Zou, W., Sitara, D., Schweitzer, M., Hu, D., Lotinun, S., Sano, Y., Baron, R., Park, J.M., et al. (2010). The p38 MAPK pathway is essential for skeletogenesis and bone homeostasis in mice. J. Clin. Invest. *120*, 2457-2473.

Harding, H.P. and Lazar, M.A. (1993). The orphan receptor Rev-erbA alpha activates transcription via a novel response element. Mol. Cell. Biol. *13*, 3113-3121.

He, Y., Lin, F., Chen, Y., Tan, Z., Bai, D., and Zhao, Q. (2015). Overexpression of the circadian clock gene Rev-erbalpha affects murine bone mesenchymal stem cell proliferation and osteogenesis. Stem Cells Dev. *24*, 1194-1204.

Iimura, T., Nakane, A., Sugiyama, M., Sato, H., Makino, Y., Watanabe, T., Takagi, Y., Numano, R., and Yamaguchi, A. (2012). A fluorescence spotlight on the clockwork development and metabolism of bone. J. Bone Miner. Metab. *30*, 254-269.

Kim, J., Jang, S., Choi, M., Chung, S., Choe, Y., Choe, H.K., Son, G.H., Rhee, K., and Kim, K. (2018). Abrogation of the circadian nuclear receptor REV-erbalpha exacerbates 6-hydroxydopamine-induced dopaminergic neurodegeneration. Mol. Cells *41*, 742-752.

Kim, J.H. and Kim, N. (2016). Signaling pathways in osteoclast differentiation. Chonnam Med. J. *52*, 12-17.

King, D.P. and Takahashi, J.S. (2000). Molecular genetics of circadian rhythms in mammals. Annu. Rev. Neurosci. *23*, 713-742.

Komori, T. (2011). Signaling networks in RUNX2-dependent bone development. J. Cell. Biochem. *112*, 750-755.

Lazar, M.A. (2016). Rev-erbs: integrating metabolism around the clock. In a Time for Metabolism and Hormones, P. Sassone-Corsi and Y. Christen, eds. (Cham, Switzerland: Springer), pp. 63-70.

Lazar, M.A., Hodin, R.A., Darling, D.S., and Chin, W.W. (1989). A novel member of the thyroid/steroid hormone receptor family is encoded by the opposite strand of the rat C-erbA alpha transcriptional unit. Mol. Cell. Biol. *9*, 1128-1136.

Lee, S.Y., Kim, G.T., Yun, H.M., Kim, Y.C., Kwon, I.K., and Kim, E.C. (2018). Tectorigenin promotes osteoblast differentiation and in vivo bone healing, but suppresses osteoclast differentiation and in vivo bone resorption. Mol. Cells *41*, 476-485.

Li, X., Liu, N., Gu, B., Hu, W., Li, Y., Guo, B., and Zhang, D. (2018). BMAL1 regulates balance of osteogenic-osteoclastic function of bone marrow mesenchymal stem cells in type 2 diabetes mellitus through the NF-kappaB pathway. Mol. Biol. Rep. *45*, 1691-1704.

Liu, A.C., Tran, H.G., Zhang, E.E., Priest, A.A., Welsh, D.K., and Kay, S.A. (2008). Redundant function of REV-ERBalpha and beta and non-essential role for Bmal1 cycling in transcriptional regulation of intracellular circadian rhythms. PLoS Genet. *4*, e1000023.

Matsumoto, M., Kogawa, M., Wada, S., Takayanagi, H., Tsujimoto, M., Katayama, S., Hisatake, K., and Nogi, Y. (2004). Essential role of p38 mitogen-activated protein kinase in cathepsin K gene expression during osteoclastogenesis through association of NFATc1 and PU.1. J. Biol. Chem. *279*, 45969-45979.

Maury, E., Hong, H.K., and Bass, J. (2014). Circadian disruption in the pathogenesis of metabolic syndrome. Diabetes Metab. *40*, 338-346.

McDearmon, E.L., Patel, K.N., Ko, C.H., Walisser, J.A., Schook, A.C., Chong, J.L., Wilsbacher, L.D., Song, E.J., Hong, H.K., Bradfield, C.A., et al. (2006). Dissecting the functions of the mammalian clock protein BMAL1 by tissue-specific rescue in mice. Science *314*, 1304-1308.

McElderry, J.D., Zhao, G., Khmaladze, A., Wilson, C.G., Franceschi, R.T., and Morris, M.D. (2013). Tracking circadian rhythms of bone mineral deposition in murine calvarial organ cultures. J. Bone Miner. Res. *28*, 1846-1854.

Ogawa, S., Lozach, J., Jepsen, K., Sawka-Verhelle, D., Perissi, V., Sasik, R., Rose, D.W., Johnson, R.S., Rosenfeld, M.G., and Glass, C.K. (2004). A nuclear receptor corepressor transcriptional checkpoint controlling activator protein 1-dependent gene networks required for macrophage activation. Proc. Natl. Acad. Sci. U. S. A. *101*, 14461-14466.

Ramakrishnan, S.N. and Muscat, G.E. (2006). The orphan Rev-erb nuclear receptors: a link between metabolism, circadian rhythm and inflammation? Nucl. Recept. Signal. *4*, e009.

Reppert, S.M. and Weaver, D.R. (2002). Coordination of circadian timing in

mammals. Nature *418*, 935-941.

Rodriguez-Carballo, E., Gamez, B., and Ventura, F. (2016). p38 MAPK signaling in osteoblast differentiation. Front. Cell. Dev. Biol. *4*, 40.

Roodman, G.D. (2006). Regulation of osteoclast differentiation. Ann. N. Y. Acad. Sci. *1068*, 100-109.

Samsa, W.E., Vasanji, A., Midura, R.J., and Kondratov, R.V. (2016). Deficiency of circadian clock protein BMAL1 in mice results in a low bone mass phenotype. Bone *84*, 194-203.

Schibler, U. and Sassone-Corsi, P. (2002). A web of circadian pacemakers. Cell *111*, 919-922.

Schroeder, T.M., Kahler, R.A., Li, X., and Westendorf, J.J. (2004). Histone deacetylase 3 interacts with runx2 to repress the osteocalcin promoter and regulate osteoblast differentiation. J. Biol. Chem. *279*, 41998-42007.

Song, C., Tan, P., Zhang, Z., Wu, W., Dong, Y., Zhao, L., Liu, H., Guan, H., and Li, F. (2018). REV-erb agonism suppresses osteoclastogenesis and prevents ovariectomy-induced bone loss partially via FABP4 upregulation. FASEB J. *32*, 3215-3228.

Sowa, H., Kaji, H., Yamaguchi, T., Sugimoto, T., and Chihara, K. (2002). Activations of ERK1/2 and JNK by transforming growth factor beta negatively regulate Smad3-induced alkaline phosphatase activity and mineralization in mouse osteoblastic cells. J. Biol. Chem. *277*, 36024-36031.

Trump, R.P., Bresciani, S., Cooper, A.W., Tellam, J.P., Wojno, J., Blaikley, J., Orband-Miller, L.A., Kashatus, J.A., Boudjelal, M., Dawson, H.C., et al. (2013). Optimized chemical probes for REV-erbalpha. J. Med. Chem. *56*, 4729-4737.

Wu, X., Yu, G., Parks, H., Hebert, T., Goh, B.C., Dietrich, M.A., Pelled, G., Izadpanah, R., Gazit, D., Bunnell, B.A., et al. (2008). Circadian mechanisms in murine and human bone marrow mesenchymal stem cells following dexamethasone exposure. Bone *42*, 861-870.

Xiao, G., Jiang, D., Gopalakrishnan, R., and Franceschi, R.T. (2002). Fibroblast growth factor 2 induction of the osteocalcin gene requires MAPK activity and phosphorylation of the osteoblast transcription factor, Cbfa1/Runx2. J. Biol. Chem. *277*, 36181-36187.

Xu, C., Ochi, H., Fukuda, T., Sato, S., Sunamura, S., Takarada, T., Hinoi, E., Okawa, A., and Takeda, S. (2016). Circadian clock regulates bone resorption in mice. J. Bone Miner. Res. *31*, 1344-1355.

Yin, L. and Lazar, M.A. (2005). The orphan nuclear receptor Rev-erbalpha recruits the N-CoR/histone deacetylase 3 corepressor to regulate the circadian Bmal1 gene. Mol. Endocrinol. *19*, 1452-1459.

Zamir, I., Zhang, J., and Lazar, M.A. (1997). Stoichiometric and steric principles governing repression by nuclear hormone receptors. Genes Dev. *11*, 835-846.

Ziros, P.G., Gil, A.P., Georgakopoulos, T., Habeos, I., Kletsas, D., Basdra, E.K., and Papavassiliou, A.G. (2002). The bone-specific transcriptional regulator Cbfa1 is a target of mechanical signals in osteoblastic cells. J. Biol. Chem. *277*, 23934-23941.

Zvonic, S., Ptitsyn, A.A., Kilroy, G., Wu, X., Conrad, S.A., Scott, L.K., Guilak, F., Pelled, G., Gazit, D., and Gimble, J.M. (2007). Circadian oscillation of gene expression in murine calvarial bone. J. Bone Miner. Res. *22*, 357-365.